Journal of Current Science and Technology, September-December 2022 Vol. 12 No. 3, pp. 505-516

ISSN 2630-0656 (Online)

Cite this article: Tansathien, K., Dechsri, K., Opanasopit, P., Nuntharatanapong, N., Sukma, M., & Rangsimawong, W. (2022, September). Investigation of lipid nanocarriers and microspicule gel for dermal delivery of porcine placenta extract. *Journal of Current Science and Technology*, *12*(3), 505-516. DOI:

Journal of Current Science and Technology

Journal homepage: https://jcst.rsu.ac.th

Investigation of lipid nanocarriers and microspicule gel for dermal delivery of porcine placenta extract

Kritsanaporn Tansathien[1, a], Koranat Dechsri[1, b], Praneet Opanasopit[1, c], Nopparat Nuntharatanapong[1, d], Monrudee Sukma[1, e], and Worranan Rangsimawong[2, f*]

[1]Department of Pharmaceutical Technology, Faculty of Pharmacy, Silpakorn University, Nakhon Pathom, 73000, Thailand
[2]Division of Pharmaceutical Chemistry and Technology, Faculty of Pharmaceutical Sciences, Ubon Ratchathani University, Ubon Ratchathani, 34190, Thailand
[a]isomeroff@gmail.com, [b]koranat_d@kkumail.com, [c]opanasopit_p@su.ac.th, [d]nuntharatanapon_n@su.ac.th, [e]Sukma_M@su.ac.th, [f]worranan.r@ubu.ac.th

*Corresponding author; E-mail: worranan.r@ubu.ac.th

Received 25 February 2022; Revised 15 August 2022; Accepted 15 August 2022;
Published online 26 December 2022

Abstract

The primary active ingredient of porcine placenta extract (PPE) is a total protein that is limited the transportation of its content into the skin. The objective was to investigate the dermal delivery of PPE using lipid nanocarriers and a microspicule (MS) gel. The liposomes (LI), PEGylated liposomes (P-LI), niosomes (NI), and PEGylated niosomes (P-NI) for loading PPE were formulated and characterized the physicochemical properties. PPE-loaded nanocarriers were added to the MS gel. The *in vitro* skin deposition study and confocal laser scanning microscopy (CLSM) were performed. For the results, all formulations were nanometers (84 to 172 nm) in size with narrow size distribution and negatively charged (-11 to -31 mV). The percent loading capacity (% LC) of NI (26.43 ± 1.69 %) was higher than that of P-NI (23.97 ± 0.55 %), LI (4.87 ± 0.13 %), and P-LI (4.25 ± 0.05 %), respectively. All nanocarriers were successfully mixed with MS gel. After applying the formulations to the skin for four hours, NI-MS gel showed significantly higher total protein deposited into the skin (345.19 ± 53.65 µg/ml) than that the gel-based formulation did (175.56 ± 67.28 µg/ml) (p<0.05). The CLSM study confirmed that the NI-MS gel could deliver bovine serum albumin-fluorescein isothiocyanate (BSA-FITC) as the macromolecular protein marker through the stratum corneum barrier into the deep skin. In conclusion, the NI-MS gel exhibited suitable physicochemical properties, suggesting that this model could play an essential role as a dermal delivery system for PPE and other macromolecules.

Keywords**:** *dermal delivery; liposome; noisome; PEGylation; microspicule; porcine placenta extract; gels.*

1. Introduction

Mammalian placentas are a rich source of biologically active substances, such as proteins, nucleic acids, amino acids, peptides, cytokines, growth factors, vitamins, and minerals (Pan, Chan, Wong, Klokol, & Chernykh, 2017). Placental extracts have been used in the cosmeceutical and pharmaceutical industries. Porcine placenta extract (PPE) increases collagen production and prevents collagen degradation by increasing skin cell proliferation and procollagen C peptide release (Hong, Park, Kim, Kim, & Suh, 2015). An *in vivo* animal study showed that delivering hydrolyzed PPE by the oral route could repair dehydration of the skin from photo-aging by increasing the water-holding capacity and reducing transepidermal water loss. In addition, the hydrolyzed PPE improved the skin damage from photo-aging by decreasing collagen

degradation (Hong et al., 2015). Recently, PPE delivered by the oral route was examined in an *in vivo* human study for its ability to improve the condition and maintain good skin quality; the oral intake of PPE supplements was shown to increase skin hydration (Nagae et al., 2020). With respect to the transdermal route, cosmetic products, such as lotions, ointments, and emulsions have been formulated to contain placenta extract (Muralidhar, & Panda, 1999). However, bioactive macromolecules from placenta extracts are limited in their permeation of the skin. To overcome this limitation, physicochemical technologies have since been developed to deliver the extracted macromolecules into the skin.

A transdermal delivery system is a non-invasive or minimally invasive technique that affords the ability of compounds to pass through the skin. This system has many advantages for the delivery of proteins when compared with the oral route such as protecting the proteins from chemical and enzymatic degradation, reducing the dose frequency, bypassing hepatic first-pass metabolism, minimizing adverse drug effects, and improving patient compliance (Bajracharya, Song, Back, & Han, 2019). The skin can be divided into three primary layers: epidermis, dermis, and hypodermis. Route of drug penetration into the skin can be separated into transepidermal and transappendageal pathways. Firstly, the main route is transepidermal, which can be subdivided into the transcellular and intercellular routes. The transcellular route primarily allows the compounds to permeate through the keratinocytes, then across the intercellular lipids. In contrast, the intercellular route is a continuous but tortuous way through the intercellular lipid domains. Secondly, the transappendageal pathway refers to drug delivery via hair follicles or sweat glands in the skin. This route is convenient for delivering macromolecular compounds (El Maghraby, Barry, & Williams, 2008; Ramadon, McCrudden, Courtenay, & Donnelly, 2022).

Peptides and proteins are typically hydrophilic macromolecules, which are limited in their transport through the epidermal layer. The stratum corneum (SC), the uppermost layer of the epidermis, and associated lipid components act as the epidermal barrier (Peña-Juárez, Guadarrama-Escobar, & Escobar-Chávez, 2022). Moreover, recent improvements in nanotechnologies, including chemical adjuvants and physical penetration enhancements, have been reported to improve the delivery of transdermal hydrophilic macromolecules using polymer-based formulations, lipid-based formulations, iontophoresis, sonophoresis, electroporation, and microneedles (An et al., 2020). Various nanocarriers, such as liposomes (LI) and niosomes (NI), have also been designed to deliver protein through the skin (Chaulagain, Jain, Tiwari, Verma, & Jain, 2018). More recently, phospholipid vesicular nanocarriers have been designed for delivering biological macromolecules. The benefit of these nanocarriers is the ability to encapsulate both hydrophilic and hydrophobic compounds, thus resulting in increased bioavailability. Modifying the surface structure using materials like polyethylene glycol (PEG) makes the nanocarriers more stable, with unique properties (Mirtaleb, Shahraky, Ekrami, & Mirtaleb, 2021). In topical pharmaceutical and cosmetic products, phospholipids are biocompatible and safe and have an efficacious interaction with dermal cells. Nanocarriers made from unsaturated phospholipids have been shown to reach the greatest relative depth of penetration into the SC (van Hoogevest, & Fahr, 2019). In addition, non-ionic surfactant-based vesicles or NI could deliver both hydrophilic and hydrophobic molecules, providing both biocompatibility and safety. They are attractive for the transportation of many compounds through the skin in the pharmaceutical and cosmetic fields (Ge, Wei, He, & Yuan, 2019). In general, traditional LI is made from phospholipids with or without steroids (e.g., cholesterol), whereas NI is formulated with non-ionic surfactants and cholesterol (Abdelkader, Alani, & Alany, 2014; Pierre, & dos Santos Miranda Costa, 2011). With respect to PEGylated nanocarriers, PEGylated liposomes (P-LI) showed that more hydrophilic sodium fluorescein penetrated the skin than that non-PEGylated liposomes did (Rangsimawong, Opanasopit, Rojanarata, Duangjit, & Ngawhirunpat, 2016).

Microdermabrasion, which requires minimal insertion into the skin and removes the SC layer, was also used to improve cutaneous drug delivery in dermatological and cosmeceutical techniques for skin regeneration. Hence, the system has been widely applied to the cosmetic field for enhancing the delivery of therapeutic compounds (Benson, Grice, Mohammed, Namjoshi, & Roberts, 2019). Furthermore, microspicules (MS) from *Spongilla lacustris* are freshwater sponge extracts that could be used in biomedical and cosmeceutical applications. The needle-like structures of MS cause microdermabrasion and create micropores in the

skin. MS effectively increased the permeation of hydrophilic macromolecules through the skin (Tansathien et al., 2019). A combination of nanocarriers and physical enhancements would effectively increase the delivery of the transdermal bioactive molecules when compared with either used alone (Yu, Yang, Wu, & Fan, 2021). However, an investigation of the dermal delivery of PPE using various lipid nanocarriers, such as LI, NI, and PEGylated nanocarriers with MS gel, has not been undertaken yet. Therefore, the dermal delivery of PPE using lipid nanocarriers and an MS gel might play an important role to deliver PPE into the skin.

2. Objectives

The aim of this study was to investigate the dermal delivery of PPE using lipid nanocarriers and an MS gel. The liposomes (LI), PEGylated liposomes (P-LI), niosomes (NI), and PEGylated niosomes (P-NI) for loading PPE were formulated and characterized the physicochemical properties. PPE-loaded nanocarriers were added to the MS gel. The *in vitro* skin deposition study and confocal laser scanning microscopy (CLSM) were performed to evaluate the transport of macromolecular protein into the skin.

3. Materials and Methods

3.1 Materials

The porcine placenta was obtained from Charnchai Farm, Ratchaburi, Thailand. Span 20, cholesterol (Chol), and bovine serum albumin-fluorescein isothiocyanate (BSA-FITC) were obtained from Sigma-Aldrich, MO, USA. Egg phosphatidylcholine (Egg PC) and N-(carbonyl-methoxypolyethyleneglycol-2000)-1,2-distearoyl-sn-glycero-3-phosphoethylene sodium salt (PEG2000-DSPE) were obtained from Lipoid GmbH, Ludwigshafen, Germany. Lissamine™ (rhodamine B 1,2-dihexadecanoylsn-glycero-3-phosphoethanolamine triethylammonium salt; Rh-PE) was obtained from Invitrogen, Carlsbad, CA, USA. *Spongilla* spicules powder (98% purity) was obtained from Hunan Sunshine Bio-Tech Co., Ltd., Hunan, China. Components for gel-based delivery (e.g., ethylenediaminetetraacetic acid disodium salt (EDTA 2Na), glycerin, Microcare® PHC, far infrared water, and SEPIMAX™ ZEN) were obtained from Zen Innovation Group Company Limited, Pathum Thani, Thailand. Other chemical agents were analytical grade.

3.2 Methods

3.2.1 Extraction of porcine placenta

The porcine placenta was washed with 0.9% w/v NaCl solution, blended into small pieces with phosphate-buffered saline (PBS pH 7.4) in a 1:1 ratio, and sonicated under an ice bath for 30 min using a probe sonicator (Vibra-Cell™, High-Intensity Ultrasonic Processors VCX500, Sonics & Materials, Newtown, CT, USA.) with a frequency of 40 kHz at 40% amplitude. The extract was centrifuged at 4,000 rpm and at a temperature of 4°C for 15 min with a centrifuge. The supernatant was collected and dried with a freeze dryer (FreeZone 2.5, Labconco, Kansas City, MO, USA) for 3 days. PPE powder was stored at 4°C until being used. Protein content was determined using the Lowry method. Briefly, 25 µl of each sample was mixed with 200 µl of alkaline solution and incubated in the dark at 25°C for 10 min. Diluted Folin's reagent (1:1) was added and the mixture was incubated at 25°C for 5 min. Protein content was measured using a microplate reader (VICTOR Nivo™ multimode plate reader, PerkinElmer, Germany) at an absorbance of 550 nm.

3.2.2 Preparation of the lipid nanocarrier formulations

The components of the lipid-based nanocarrier formulations loading on the PPE are shown in Table 1. All formulations were performed by thin-film hydration and probe sonication methods (Pengnam et al., 2019; Tansathien et al., 2021). The lipid components of LI and P-LI were dissolved in a 2:1 chloroform: methanol mixture, while the lipid and surfactant components of NI and P-NI were dissolved in a 1:1 chloroform: methanol mixture. The mixture was added to the test tube and blown with nitrogen gas to evaporate the solvent, which was followed by being placed in a desiccator for over 6 h. The PPE dissolved in the water was added to a thin film to produce hydrated lipid nanovesicles. The size of the vesicles was then reduced with a probe sonicator (Vibra-Cell™, High-Intensity Ultrasonic Processors VCX500, Sonics & Materials, Newtown, CT, USA.) with a frequency of 20 kHz and 30% amplitude in an ice bath for 30 min for two cycles. The formulations were centrifuged at 15,000 rpm and a temperature of 4°C for 15 min to precipitate the unformed lipid vesicles and stored in a refrigerator (4–8°C) for the next experiments.

Table 1 The components of the lipid-based nanocarrier formulations (% w/v)

Formulations	Egg PC	Chol	Span 20	PEG2000-DSPE	PPE
LI	0.77	0.12	-	-	0.1
P-LI	0.74	0.12	-	0.04	0.1
NI	-	0.39	0.35	-	0.1
P-NI	-	0.39	0.35	0.17	0.1

3.2.3 Characterization of the lipid nanocarriers

Vesicle size, polydispersity index (PDI), and zeta potential were analyzed by an instrument that measures particle size and zeta potential (Zetasizer Nano-ZS, Malvern, Worcestershire, UK) with a 4 mW HeNe laser at a scattering angle of 173°. The nanocarriers were diluted in a ratio of 1:20 and measured in triplicate.

Centrifugal filter devices (Amicon® Ultra 100K, Merck, USA) were used for the evaluation of the percent entrapment efficiency (% EE) and loading capacity (% LC). Briefly, 2 ml of each sample was added to the device; the device was then centrifuged at 4,000 rpm at a temperature of 4°C for 15 min. The PPE-loaded nanocarriers were in the filter section. After that, 0.1% Triton X-100 was added to the vesicles in a ratio of 1:1 to break the vesicles. The total protein content as a bioactive marker was determined as described above. The % EE and % LC was calculated as Equation 1 and 2.

$$\% \text{ EE} = \frac{\text{PPE entrapped in nanocarriers}}{\text{Initial PPE loading}} \text{x} 100 \quad (1)$$

$$\% \text{ LC} = \frac{\text{PPE entrapped in nanocarriers}}{\text{Total materials of the nanocarriers}} \text{x} 100 \quad (2)$$

3.2.4 Preparation of the lipid nanocarriers in MS gel

Each lipid nanocarrier formulation was mixed with ethylenediaminetetraacetic acid disodium salt (EDTA 2Na; 0.05% w/v), glycerin (4% w/v), Microcare® PHC (0.80% v/v), far infrared water (5% v/v), and polyacrylate crosspolymer-6 (SEPIMAX™ ZEN; 0.54% w/v) to produce a gel formulation. Five milliliters of MS (1% w/w) were added to the formulation.

3.2.5 *In vitro* skin deposition study

Abdominal neonatal porcine skins were obtained from Charnchai Farm in Ratchaburi, Thailand. The thickness of the skin was approximately 0.6 to 0.7 mm without the subcutaneous fat. The protein extracted from the PPE deposited in the skin was measured using Franz diffusion cells. One gram of each formulation was added to the acceptor part of the cell; the MS formulation was gently massaged onto the skin for 2 min (approximately 160 rubbing times/1.96 cm^2 of skin area) using the forefinger with a medical glove. Six milliliters of PBS were added to the receptor at a temperature of 32°C and frequently stirred at 500 rpm. The treated skins were collected at 4 h and extracted using a probe sonicator with a frequency of 40 kHz and a 40% amplitude for 10 min under cold conditions. After that, the samples were centrifuged at 5,000 rpm for 5 min and collected from the supernatant. The protein content was analyzed with the Lowry method as described above and calculated according to the standard curve.

3.2.6 CLSM study

BSA-FITC, as a green fluorescent substance, was a model protein. Rh-PE, as a red fluorescent probe, was grafted to the membrane of the lipid nanocarriers. After Rh-PE permeated the skin for 4 h, the treated skins were washed with PBS and methyl salicylate was added. The skins were observed with CLSM using an inverted Zeiss LSM 800 microscope (Carl Zeiss, Jena, Germany) equipped with HeNe (excitation wavelength 543 nm; emission wavelength 580 nm), Ar (excitation 488 nm; emission 514 nm), and diode lasers (excitation 358 nm; emission 461 nm). The results were visualized using a × 10 objective lens and presented as x–z axis serial optical sections. Each image was evaluated at the middle horizontal line. The result was graphed as the profile of the mean fluorescence intensity versus skin depth.

3.2.7 Statistical analysis

All experiments were performed in triplicate. The data are reported as the mean ± standard deviation (SD). The analytic statistic was determined using one-way ANOVA with a post hoc test and Student's t-test. The values were presented as significantly different when $p < 0.05$.

4. Results and Discussion

4.1 Physicochemical properties of the PPE-loaded nanocarriers

PPE had a brown-red fibrous texture, and the total protein content was 0.150 ± 0.003 g/g of dry extract. After loading onto the lipid nanocarriers, the vesicle size, size distribution, and surface charge of the nanocarriers presented with nanometer sizes and narrow size distribution (PDI < 0.3); the liposomal vesicles were smaller than the niosomal ones. Liposomal vesicles are organized from double-chain phospholipid and lipid agents, resulting in small (<100 nm), unilamellar vesicles being expressed. Conversely, niosomal vesicles are formed from a non-ionic single-chain surfactant (Span 20) and lipid component. The size of niosomes depends on alkyl chain length, resulting in large (100–250 nm), unilamellar vesicles being expressed (Gharbavi, Amani, Kheiri-Manjili, Danafar, & Sharafi, 2018). The surface charge of the LI formulations was between -11 and -12 mV, whereas the NI formulations were negatively charged in the range of -20 to -32 mV. The zeta potentials in both types of LI were negative because Egg PC is a zwitterionic substance. When the pH of the formulations was 7.4, higher than the isoelectric point (pI) of PC (pH 6.0–6.7), the vesicles carried a negative charge (Rangsimawong et al., 2016). For the NI formulations, the zeta potentials were more negative than those of the liposomes because the composition of the nanocarriers resulted in the surface charge. In a previous report, LI composed of phospholipid and cholesterol was less negative than NI with a non-ionic surfactant (Ghanbarzadeh, Khorrami, & Arami, 2015). Moreover, the PEG2000-DSPE grafted nanocarriers could reduce the negative surface charge, suggesting that the surface charge depended on the acidic or basic strengths of the surface groups and the pH of the medium. The pH of the formulations was 7.4; thus, the basic surface took on a positive charge, resulting in decreasing the negative charge on the PEGylated LI and NI (Okore, Attama, Ofokansi, Esimone, & Onuigbo, 2011; Rangsimawong et al., 2016). Generally, PEG acts as a steric stabilizer of the nanocarrier structure, leading to reduce protein degradation, increase hydrophilic properties, and improving the capability of protein delivery (Huang, Chen, Chen, Gao, & Liang, 2008). Total protein content was used as a bioactive marker of PPE in the nanocarriers. The % EE of nanocarriers showed that LI had the highest value at 40%, followed by P-LI, P-NI, and NI. NI had higher % LC values than P-NI, LI, and P-LI. Cholesterol is an amphiphilic molecule that can combine with surfactant. Thus, it can increase the rigidity of vesicles, membrane transaction, and membrane leakage, suggesting that the cholesterol enhances the entrapment efficiency. In this study, the cholesterol concentrations in LI and P-LI were higher than in NI and P-NI and the % EE values of LI and P-LI were higher than in NI and P-NI. As the result, the % LC of all formulations was lower than % EE because of the total nanocarrier weight of each formulation. The total weights of NI and P-NI were less than those of LI and P-LI, leading to the % LC values of NI and P-NI being higher (Gharbavi et al., 2018). Cost-effectiveness is an important factor when formulating cosmeceutical products and the components of LI, P-LI, and P-NI are expensive. Thus, NI was selected to develop the gel-based nanocarrier formulation for delivering PPE through the skin. The results were shown in Table 2.

Table 2 The physicochemical properties of the lipid nanocarrier formulations

Formulations	Size (nm)	PDI	Zeta potential (mV)	% EE	% LC
LI	85.46 ± 0.44	0.221 ± 0.01	-11.87 ± 0.67	40.17 ± 1.08	4.87 ± 0.13
P-LI	84.02 ± 0.52	0.190 ± 0.01	-12.03 ± 0.49	39.50 ± 0.32	4.25 ± 0.05
NI	145.30 ± 1.61	0.248 ± 0.01	-31.60 ± 1.35	24.18 ± 1.67	26.43 ± 1.69
P-NI	172.70 ± 0.27	0.241 ± 0.01	-20.67 ± 0.29	26.88 ± 0.74	23.97 ± 0.55

The results are presented as the mean ± standard deviation (SD) (n=3).

The nanocarrier solutions were prepared by adding a gelling agent to the nanocarrier to form a semi-solid matrix under gentle homogenization. With respect to the gel components, glycerin is an emollient for reducing moisture evaporation, whereas EDTA 2Na is a chelating agent and Microcare® PHC is a preservative that increase the stability of the formulation. Far infrared water is a technology used to improve the absorption of the compound into the skin. SEPIMAX™ ZEN is a thickening agent. With respect to the gel-based nanocarriers, all formulations had suitable

appearances and there were no coarse particles in the gel. Moreover, the high viscosity of the gel offered superior stability to suspend the macromolecules, nanocarriers, and MS than the solution alone. The polymeric gel promoted a steric effect and avoided the fusion of the nanocarriers without any interaction together. The polymeric gel promoted a steric effect and avoided the fusion of the nanocarriers without any interaction together (Nigro, Cerqueira Pinto, dos Santos, & Mansur, 2020). Our previous study showed that the macromolecular protein of deer antler velvet extract-loaded NI vesicles was able to mix with MS gel. Although the nanovesicles in gel base were detected at a larger size and higher size distribution than in solution form, these vesicles were still nanometer size of vesicles. This suggested that different-sized fractions of gel base occurred. However, no coarse particles were observed in the gel formulation (Tansathien et al., 2021).

4.2 Skin deposition study

The combination of strategies to improve skin delivery (lipid nanocarrier technologies and minimally invasive delivery using MS) overcame the cutaneous limitation and expanded the ability to deliver bioactive macromolecules from the PPE via the skin. As seen in Figure 1, the protein deposited on the skin after *in vitro* cutaneous permeation for 4 h revealed that more protein was deposited onto the skin with all nanocarrier formulations than with the control (gel-based) formulation, whereas more protein was deposited with the NI-MS than with the other formulations. With respect to the mechanism by which the nanocarriers provide transdermal drug delivery, LI and NI can penetrate the skin via the transepidermal and transappendageal routes. The PEG molecule can hydrate the skin as well as change the water gradient, leading to an increase the skin permeation (Wang et al., 2017). Besides, PEG2000-DSPE might increase the elasticity of lipid-bilayer because of the characteristics of the PEG chain (Zheng et al., 2020). Additionally, the non-ionic surfactant in NI and P-NI acts as a chemical enhancer that can interact with SC components, change the structural organization of lipid bilayers, and improve skin hydration. These effects may be caused by niosomal formulations transporting the PPE greater than liposomal formulations (Cristiano, Cilurzo, Carafa, & Paolino, 2018). In addition, % LC is an indicator of the drug content, which can be encapsulated in the amount of nanocarriers weight. The higher % LC value can provide a better drug reservoir system (Massella, Leone, Peila, Barresi, & Ferri, 2018). Moreover, nanocarriers with MS gel showed higher protein deposited onto the skin than that without MS, thus indicating that the mechanisms of the MS were resurfacing the SC, creating pores, and insertion into the skin, followed by the transportation of bioactive macromolecules. Since Zhai, Zhang, Ou, and Chen (2021) has explained that the effectiveness of a skin permeation enhancement strategy of the sponge spicules was associated with the disturbances in the SC (Zhai et al., 2021). The MS created micron-scale holes in the SC to enhance the skin absorption and transdermal delivery of the hydrophilic macromolecules (Zhang et al., 2019; Liang, Zhang, Ou, Chen, Mitragotri, & Chen, 2020). Furthermore, NI with MS serum was reported to improve the skin permeation of the hydrophilic macromolecule BSA-FITC (Tansathien et al., 2021). More protein was deposited in the skin with NI than with other formulations, suggesting that the highest PPE loading capacity of NI affected the ability to deliver protein from the PPE into the skin. Therefore, NI-MS gel was appropriate to use as the dermal delivery system of PPE.

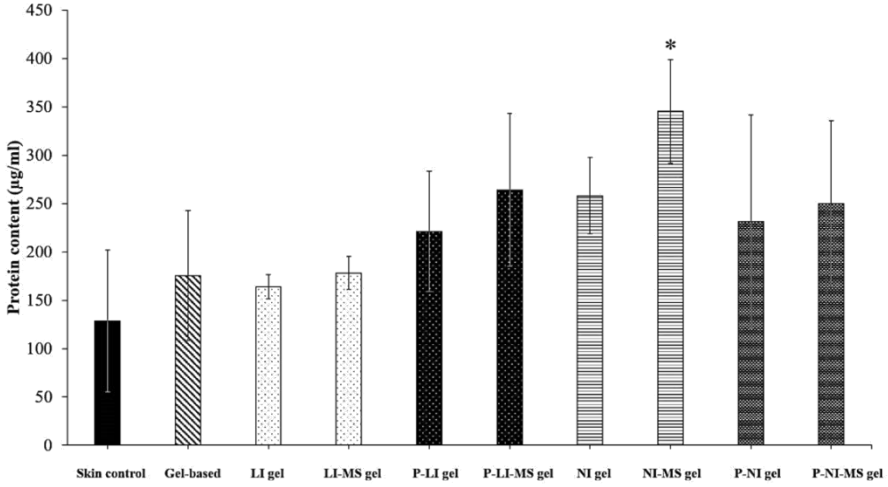

Figure 1 Protein deposited in the skin after being applied with various formulations for 4 h. * represents a significant difference from that in the gel-based formulation ($p < 0.05$) (n=3).

4.3 CLSM study

The transdermal route is advantageous for drug transportation, but the skin structure has a barrier function to limit the compounds passing through it. The SC is the main barrier for external substances, especially macromolecular compounds. The development of a novel formulation was proposed to overcome the SC barrier and enhance the permeability of the macromolecular compounds (Rabiei, Kashanian, Samavati, Jamasb, & McInnes, 2020). In the past decade, the CLSM technique can apply to visualize the transdermal delivery potential of drug-encapsulated nanocarriers as the interaction of nanocarriers with skin and their penetration pathways (Chaturvedi, & Garg, 2021). In this study, the NI-MS gel formulation exhibited the suitable physicochemical properties and the most macromolecular protein delivered into the skin. To investigate the penetration mechanism of this formulation, a CLSM technique was performed to obtain high-resolution images and visualize the distribution and skin penetration depth of the delivered drugs, presenting the ability of the NI-MS gel as a dermal delivery system of the macromolecular protein (Alvarez-Román, Naik, Kalia, Fessi, & Guy, 2004). The main active ingredient in PPE was the total protein content, whereas BSA is generally used as a protein marker in many studies. For the CLSM study, fluorescein is the most often used fluorophore for labeling proteins and the fluorescently-labeled BSA (BSA-FITC) is normally used as a fluorescent marker (Yang, Bai, & Sun, 2008). As shown in Figure 2, BSA-FITC was used as a model macromolecular protein loaded into the formulation, whereas Rh-PE was used as a fluorescent dye to probe the NI vesicles. The NI-MS gel delivered the macromolecular protein, BSA-FITC, into the skin to a depth of 90 µm (with maximum intensity at the 20 µm-depth) after treatment for 4 h; Rh-PE grafted on the surface of NI was deposited at the same area of BSA-FITC. This indicated that the NI vesicles and BSA-FITC co-migrated through the SC.

The outermost layer of the epidermis, the SC barrier, was approximately 10–20 µm thick, and the viable epidermis was 50–100 µm thick. After passing through the epidermal layers, the drugs could interact with the network of blood vessels in the dermis and be delivered to the rest of the body (Walters, 2002). This result showed the ability of the NI-MS gel to deliver the macromolecular protein through the SC and into the viable epidermis. Furthermore, NI vesicles offered high physicochemical stability and great availability of surfactant classes and enhanced the penetration of the entrapped substances across the skin (Manconi, Sinico, Valenti, Lai, & Fadda, 2006). Non-ionic surfactant (Span 20), as a chemical penetration enhancer in the NI, could enhance the skin penetration by partitioning into or interacting with the components of the SC, thus leading to changing the organization of the lipid bilayer structure and improving the skin permeability and diffusion coefficient of the drugs (Münch, Wohlrab, & Neubert, 2017). However, only the NI vesicles showed lower protein deposition into the skin than

that with MS (Figure 1). A previous study reported that the NI vesicles were unable to form vesicles within the skin and the entrapped drugs could be released from the nanocarriers before permeation through the skin (Rangsimawong, Opanasopit, Rojanarata, Panomsuk, & Ngawhirunpat, 2017). Thus, the combination of the penetration enhancing techniques could strongly improve the delivery of the macromolecular proteins into the skin.

In addition, micro-needling or laser resurfacing created the transportation routes for macromolecules, i.e., proteins and polypeptides, through the skin (Hsiao, Yang, Alalaiwe, & Fang, 2019; Kirkby, Hutton, & Donnelly, 2020). The micrometer-sized *Spongilla* spicules in the extract had a needle-like appearance, with the tip growing from two opposite sides (approximately 176.77 µm-length and 11.89 µm-diameter). *Spongilla* spicules improved the transdermal delivery of macromolecules by the dermabrasion technique (Tansathien et al., 2019). Moreover, MS could physically disrupt the skin barriers, consequently leading to enhancing the penetration of the NI vesicles and hydrophilic macromolecular proteins into the skin. Therefore, the NI-MS gel acted as a model dermal delivery system for macromolecular proteins and PPE.

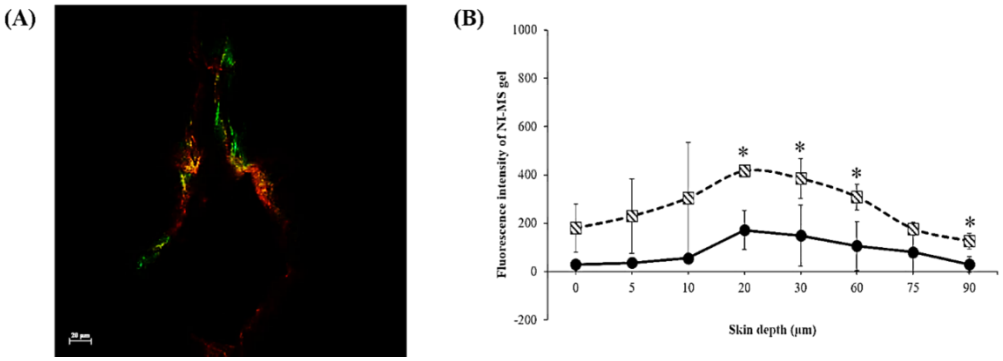

Figure 2 (A) CLSM images of porcine skin treated with bovine serum albumin-fluorescein isothiocyanate (BSA-FITC)-loaded and rhodamine B 1,2-dihexadecanoylsn-glycero-3-phosphoethanolamine triethylammonium salt (Rh-PE)-probed NI-MS gel at a time of 4 h. **(B)** fluorescence intensity profile of BSA-FITC (—●—) and Rh-PE (--▧--) from the NI-MS gel deposited in the different skin depths at 4 h. * represents a significant difference compared with the 0 µm-skin depth ($p < 0.05$) (n=3).

5. Conclusion

PPE with a high total protein content was successfully loaded into lipid nanocarrier formulations such as LI, P-LI, NI, and P-NI. All formulations exhibited a nanometer size, narrow size distribution, and negative surface charge. NI, which was prepared from Span 20 and Chol, had the highest extracted protein content loaded into the carriers from the highest value of % LC. The NI-MS gel was an appropriate appearance and had no coarse particles. A dermabrasion technique using *Spongilla* spicules or MS mixed with a nanocarrier formulation and prepared as a gel formulation was performed to enhance skin permeability. The NI-MS gel had the highest protein content deposited in the skin at four hours. Besides, a CLSM study using BSA-FITC as a protein marker confirmed that the NI-MS gel formulation delivered the protein into the skin. The NI-MS gel could transport the macromolecular protein into the skin to a depth of 90 µm after application for four hours. It can explain that MS disrupted the SC and NI vesicles with BSA-FITC co-migrated passed the SC. Therefore, the NI-MS gel played an important role as the dermal delivery system for PPE and other macromolecules.

6. Acknowledgements

The authors would like to acknowledge the financial support from the Thailand Research Fund through the Golden Jubilee Ph.D. Program (Grant No. PHD/0192/2561), National Research Council of Thailand (NRCT: N42A650551), and Office of National Higher Education Science Research and Innovation Policy Council (NXPO) through the Program Management Unit for Competitiveness (C10F640021). Furthermore, we appreciate Charnchai Farm, Ratchaburi for their support by

providing the porcine placenta and the naturally dead neonatal porcine skins, and the Zen Innovation Group Company Limited for the constituents of serum and spicules.

7. References

Abdelkader, H., Alani, A. W. G., & Alany, R. G. (2014). Recent advances in non-ionic surfactant vesicles (niosomes): self-assembly, fabrication, characterization, drug delivery applications and limitations. *Drug Delivery*, *21*(2), 87-100. https://doi.org/10.3109/10717544.2013.838077

Alvarez-Román, R., Naik, A., Kalia, Y. N., Fessi, H., & Guy, R. H. (2004). Visualization of skin penetration using confocal laser scanning microscopy. *European Journal of Pharmaceutics and Biopharmaceutics*, *58*(2), 301-316. https://doi.org/10.1016/j.ejpb.2004.03.027

An, Y.-H., Park, M. J., Lee, J., Ko, J., Kim, S.-H., Kang, D. H., & Hwang, N. S. (2020). Recent advances in the transdermal delivery of protein therapeutics with a combinatorial system of chemical adjuvants and physical penetration enhancements. *Advanced Therapeutics*, *3*(2), 1900116. https://doi.org/10.1002/adtp.201900116

Bajracharya, R., Song, J. G., Back, S. Y., & Han, H. K. (2019). Recent advancements in non-invasive formulations for protein drug delivery. *Computational and Structural Biotechnology Journal*, *17*, 1290-1308. https://doi.org/10.1016/j.csbj.2019.09.004

Benson, H. A. E., Grice, J. E., Mohammed, Y., Namjoshi, S., & Roberts, M. S. (2019). Topical and transdermal drug delivery: from simple potions to smart technologies. *Current Drug Delivery*, *16*(5), 444-460. https://doi.org/10.2174/1567201816666190201143457

Chaturvedi, S., & Garg, A. (2021). An insight of techniques for the assessment of permeation flux across the skin for optimization of topical and transdermal drug delivery systems. *Journal of Drug Delivery Science and Technology*, *62*, 102355. https://doi.org/https://doi.org/10.1016/j.jddst.2021.102355

Chaulagain, B., Jain, A., Tiwari, A., Verma, A., & Jain, S. K. (2018). Passive delivery of protein drugs through transdermal route. *Artificial Cells, Nanomedicine, and Biotechnology*, *46*(sup1), 472-487. https://doi.org/10.1080/21691401.2018.1430695

Cristiano, M. C., Cilurzo, F., Carafa, M., & Paolino, D. (2018). Chapter 4 - Innovative vesicles for dermal and transdermal drug delivery. In A. M. Grumezescu (Ed.), *Lipid Nanocarriers for Drug Targeting*. Newyork, US: William Andrew Publishing. https://doi.org/https://doi.org/10.1016/B978-0-12-813687-4.00004-9

El Maghraby, G. M., Barry, B. W., & Williams, A. (2008). Liposomes and skin: from drug delivery to model membranes. *European journal of pharmaceutical sciences*, *34*(4-5), 203-222. https://doi.org/10.1016/j.ejps.2008.05.002

Ge, X., Wei, M., He, S., & Yuan, W.-E. (2019). Advances of non-ionic surfactant vesicles (niosomes) and their application in drug delivery. *Pharmaceutics*, *11*(2), 55. https://doi.org/10.3390/pharmaceutics11020055

Ghanbarzadeh, S., Khorrami, A., & Arami, S. (2015). Nonionic surfactant-based vesicular system for transdermal drug delivery. *Drug Delivery*, *22*(8), 1071-1077. https://doi.org/10.3109/10717544.2013.873837

Gharbavi, M., Amani, J., Kheiri-Manjili, H., Danafar, H., & Sharafi, A. (2018). Niosome: a promising nanocarrier for natural drug delivery through blood-brain barrier. *Advances in Pharmacological Sciences*, *2018*, 6847971. https://doi.org/10.1155/2018/6847971

Hong, K.-B., Park, Y., Kim, J. H., Kim, J. M., & Suh, H. J. (2015). Effects of porcine placenta extract ingestion on ultraviolet B-induced skin damage in hairless mice. *Korean journal for food science of animal resources*, *35*(3), 413-420. https://doi.org/10.5851/kosfa.2015.35.3.413

Hsiao, C. Y., Yang, S. C., Alalaiwe, A., & Fang, J. Y. (2019). Laser ablation and topical drug

delivery: a review of recent advances. *Expert Opinion on Drug Delivery*, *16*(9), 937-952. https://doi.org/10.1080/17425247.2019.1649655.

Huang, Y., Chen, J., Chen, X., Gao, J., & Liang, W. (2008). PEGylated synthetic surfactant vesicles (Niosomes): novel carriers for oligonucleotides. *Journal of Materials Science: Materials in Medicine*, *19*(2), 607-614. https://doi.org/10.1007/s10856-007-3193-4

Kirkby, M., Hutton, A. R. J., & Donnelly, R. F. (2020). Microneedle mediated transdermal delivery of protein, peptide and antibody based therapeutics: current status and future considerations. *Pharmaceutical Research*, *37*(6), 117. https://doi.org/10.1007/s11095-020-02844-6

Liang, X., Zhang, J., Ou, H., Chen, J., Mitragotri, S., & Chen, M. (2020). Skin delivery of siRNA using sponge spicules in combination with cationic flexible liposomes. *Mol. Ther. Nucleic Acids*, *20*, 639-648. https://doi.org/10.1016/j.omtn.2020.04.003

Manconi, M., Sinico, C., Valenti, D., Lai, F., & Fadda, A. M. (2006). Niosomes as carriers for tretinoin: III. A study into the in vitro cutaneous delivery of vesicle-incorporated tretinoin. *International journal of pharmaceutics*, *311*(1-2), 11-19. https://doi.org/10.1016/j.ijpharm.2005.11.045

Massella, D., Leone, F., Peila, R., Barresi, A. A., & Ferri, A. (2018). Functionalization of cotton fabrics with polycaprolactone nanoparticles for transdermal release of melatonin. *Journal of Functional Biomaterials*, *9*(1), 1-15. https://doi.org/10.3390/jfb9010001

Mirtaleb, M. S., Shahraky, M. K., Ekrami, E., & Mirtaleb, A. (2021). Advances in biological nano-phospholipid vesicles for transdermal delivery: A review on applications. *Journal of Drug Delivery Science and Technology*, *61*, 102331. https://doi.org/https://doi.org/10.1016/j.jddst.2021.102331

Münch, S., Wohlrab, J., & Neubert, R. H. H. (2017). Dermal and transdermal delivery of pharmaceutically relevant macromolecules. *European Journal of Pharmaceutics and Biopharmaceutics*, *119*, 235-242. https://doi.org/10.1016/j.ejpb.2017.06.019

Muralidhar, R. V., & Panda, T. (1999). Useful products from human placenta. *Bioprocess Engineering*, *20*(1), 23-25. https://doi.org/10.1007/s004490050554

Nagae, M., Nagata, M., Teramoto, M., Yamakawa, M., Matsuki, T., Ohnuki, K., & Shimizu, K. (2020). Effect of porcine placenta extract supplement on skin condition in healthy adult women: a randomized, double-blind placebo-controlled study. *Nutrients*, *12*(6), 1671. https://doi.org/10.3390/nu12061671

Nigro, F., Cerqueira Pinto, C. D. S., dos Santos, E. P., & Mansur, C. R. E. (2022). Niosome-based hydrogel as a potential drug delivery system for topical and transdermal applications. *International Journal of Polymeric Materials and Polymeric Biomaterials*, *71*(6), 444-461. https://doi.org/10.1080/00914037.2020.1848833

Okore, V. C., Attama, A. A., Ofokansi, K. C., Esimone, C. O., & Onuigbo, E. B. (2011). Formulation and evaluation of niosomes. *Indian journal of pharmaceutical sciences*, *73*(3), 323-328. https://doi.org/10.4103/0250-474X.93515

Pan, S. Y., Chan, M. K. S., Wong, M. B. F., Klokol, D., & Chernykh, V. (2017). Placental therapy: an insight to their biological and therapeutic properties. *Journal of Medicine and Therapeutics*, *1*(3), 1-6. https://doi.org/10.15761/JMT.1000118

Peña-Juárez, M., Guadarrama-Escobar, O. R., & Escobar-Chávez, J. J. (2022). Transdermal delivery systems for biomolecules. *Journal of Pharmaceutical Innovation*, *17*(2), 319-332. https://doi.org/10.1007/s12247-020-09525-2

Pengnam, S., Patrojanasophon, P., Rojanarata, T., Ngawhirunpat, T., Yingyongnarongkul, B. E., Radchatawedchakoon, W., & Opanasopit, P. (2019). A novel plier-like gemini cationic niosome for nucleic acid delivery. *Journal of Drug Delivery Science and Technology*, *52*, 325-333. https://doi.org/10.1016/j.jddst.2019.04.032

Pierre, M. B. R., & dos Santos Miranda Costa, I. (2011). Liposomal systems as drug delivery vehicles for dermal and transdermal applications. *Archives of Dermatological Research*, *303*(9), 607. https://doi.org/10.1007/s00403-011-1166-4

Rabiei, M., Kashanian, S., Samavati, S. S., Jamasb, S., & McInnes, S. J. P. (2020). Nanomaterial and advanced technologies in transdermal drug delivery. *Journal of Drug Targeting*, *28*(4), 356-367. https://doi.org/10.1080/1061186X.2019.1693579

Ramadon, D., McCrudden, M. T., Courtenay, A. J., & Donnelly, R. F. (2022). Enhancement strategies for transdermal drug delivery systems: Current trends and applications. *Drug Delivery and Translational Research*, *12*(4), 758-791. https://doi.org/10.1007/s13346-021-00909-6

Rangsimawong, W., Opanasopit, P., Rojanarata, T., Panomsuk, S. & Ngawhirunpat, T. (2017). Influence of sonophoresis on transdermal drug delivery of hydrophilic compound-loaded lipid nanocarriers. *Pharmaceutical Development and Technology*, *22*(4), 597-605. https://doi.org/10.1080/10837450.2016.1221428

Rangsimawong, W., Opanasopit, P., Rojanarata, T., Duangjit, S., & Ngawhirunpat, T. (2016). Skin transport of hydrophilic compound-loaded PEGylated lipid nanocarriers: comparative study of liposomes, niosomes, and solid lipid nanoparticles. *Biological and Pharmaceutical Bulletin*, *39*(8), 1254-1262. https://doi.org/10.1248/bpb.b15-00981

Tansathien, K., Chareanputtakhun, P., Ngawhirunpat, T., Opanasopit, P., & Rangsimawong, W. (2021). Hair growth promoting effect of bioactive extract from deer antler velvet-loaded niosomes and microspicules serum. *International Journal of Pharmaceutics*, *597*, 120352. https://doi.org/10.1016/j.ijpharm.2021.120352

Tansathien, K., Suriyaaumporn, P., Charoenputtakhun, P., Ngawhirunpat, T., Opanasopit, P., & Rangsimawong, W. (2019). Development of sponge microspicule cream as a transdermal delivery system for protein and growth factors from deer antler velvet extract. Biological and Pharmaceutical Bulletin, 42(7), 1207-1215. https://doi.org/10.1248/bpb.b19-00158

van Hoogevest, P., & Fahr, A. (2019). *Phospholipids in cosmetic carriers*. In J. Cornier, C. M. Keck, & M. Van de Voorde (Eds.), Nanocosmetics: From Ideas to Products. New York, US: Springer International Publishing. https://doi.org/10.1007/978-3-030-16573-4_6

Walters, K. A. (2002). The structure and Function of Skin. *Dermatological and Transdermal Formulation*. (Walters KA, Robert MS eds.) Florida, US: CRC Press.

Wang, J., Wei, Y., Fei, Y. R., Fang, L., Zheng, H. S., Mu, C. F., ... & Zhang, Y. S. (2017). Preparation of mixed monoterpenes edge activated PEGylated transfersomes to improve the in vivo transdermal delivery efficiency of sinomenine hydrochloride. *International Journal of Pharmaceutics*, *533*(1), 266-274. https://doi.org/https://doi.org/10.1016/j.ijpharm.2017.09.059

Yang, K., Bai, S., & Sun, Y. (2008). Protein adsorption dynamics in cation-exchange chromatography quantitatively studied by confocal laser scanning microscopy. *Chemical Engineering Science*, *63*(16), 4045-4054. https://doi.org/https://doi.org/10.1016/j.ces.2008.05.013

Yu, Y. Q., Yang, X., Wu, X. F., & Fan, Y. B. (2021). Enhancing permeation of drug molecules across the skin via delivery in nanocarriers: novel strategies for effective transdermal applications. *Frontiers in Bioengineering and Biotechnology*, *9*, 646554. https://doi.org/10.3389/fbioe.2021.646554

Zhai, H., Zhang, C., Ou, H., & Chen, M. (2021). Transdermal delivery of heparin using low-frequency sonophoresis in combination with sponge spicules for venous thrombosis treatment. *Biomaterials Science*, *9*(16), 5612-5625. https://doi.org/10.1039/D1BM00703C

Zhang, C., Zhang, K., Zhang, J., Ou, H., Duan, J., Zhang, S., ... & Chen, M. (2019). Skin

delivery of hyaluronic acid by the combined use of sponge spicules and flexible liposomes. *Biomater. Sci.*, *7*(4), 1299-1310. https://doi.org/10.1039/C8BM01555D

Zheng, H., Xu, C., Fei, Y., Wang, J., Yang, M., Fang, L., ... & Tao, C. (2020). Monoterpenes-containing PEGylated transfersomes for enhancing joint cavity drug delivery evidenced by CLSM and double-sited microdialysis. *Materials Science and Engineering: C*, *113*, 110929. https://doi.org/https://doi.org/10.1016/j.msec.2020.110929

Supplement

The following Table describes the various abbreviations used throughout the study. Nonstandard abbreviations that are used to abbreviate the names are written in this list.

Abbreviation	Meaning
BSA-FITC	Bovine serum albumin-fluorescein isothiocyanate
Chol	Cholesterol
CLSM	Confocal laser scanning microscopy
EDTA 2Na	Ethylenediaminetetraacetic acid disodium salt
%EE	Percent entrapment efficiency
Egg PC	Egg phosphatidylcholine
%LC	Percent loading capacity
LI	Liposomes
MS	Microspicule
NI	Niosomes
PBS	Phosphate-buffered saline
PDI	Polydispersity index
PEG	Polyethylene glycol
PEG2000-DSPE	N-(carbonyl-methoxypolyethyleneglycol-2000)-1,2-distearoyl-sn-glycero-3-phosphoethylene sodium salt
pI	Isoelectric point
P-LI	Pegylated liposomes
P-NI	Pegylated niosomes
PPE	Porcine placenta extract
Rh-PE	Rhodamine B 1,2-dihexadecanoylsn-glycero-3-phosphoethanolamine triethylammonium salt
SC	Stratum corneum
SD	Standard deviation